Available online at www.sciencedirect.com
SCIENCE DIRECT®
Polymer 44 (2003) 4715–4721
polymer
www.elsevier.com/locate/polymer

Permeability of polyimides derived from non-coplanar diamines and 4,4′-(hexafluoroisopropylidene)diphthalic anhydride

J.W. Xu[a], M.L. Chng[b], T.S. Chung[b,*], C.B. He[a], R. Wang[c]

[a]*Institute of Materials Research and Engineering, 3 Research Link, Singapore 117602*
[b]*Department of Chemical Engineering, National University of Singapore, 10 Kent Ridge Crescent, Singapore 119260*
[c]*Institute of Environmental Science and Technology (IESE), 18 Nanyang Drive, Singapore 637723*

Received 16 December 2002; received in revised form 17 March 2003; accepted 5 May 2003

Abstract

A series of polyimides including a non-coplanar moiety were synthesized in order to investigate the effect on gas permeability and selectivity. The gas permeation properties of He, H_2, O_2, N_2, CH_4 and CO_2 were measured using a constant-volume method. Only 6FDA-terphenyl consisting of laterally attached phenyl groups shows a substantial increase because its terphenyl moiety is a rigid structure with a high aspect ratio. The order of permeability increase from 6FDA-phenyl to 6FDA-terphenyl is consistent with the calculated fraction free volume and measured permittivity. It is observed that the most gain in permeability for 6FDA-terphenyl polyimide arises from the enhancement in apparent diffusion coefficient, while the permeability increase for 6FDA-biphenyl is mainly due to the increase in solubility. A relationship of diffusivity vs. gas penetrant size as well as gas solubility vs. critical temperature of gas penetrant was also investigated.

Keywords: 6FDA-polyimide; Permeability; Gas separation

1. Introduction

Aromatic polyimides are one of the most useful and important polymers because of their excellent thermal stability, good chemical resistance, mechanical strength and low dielectric constants. They have been widely used in microelectronic, aviation, defense, and separation industries. When using polyimides as a membrane material for gas separation, their low permeability and relatively less tractability restrict their full potential. Many efforts have been made to synthesize organosoluble polyimides by incorporating different moieties to enhance their intrinsic permeability and tractability [1–5]. A desirable gas separation membrane material should possess inherent characteristics of high permeability and permselectivity as well as good processibility.

In the polyimide family, fluoro-polyimides containing 4,4′-(hexafluoroisopropylidene) diphthalic anhydride (6FDA) have been identified as a material having great potential for gas separation. This is because the rigid molecular structure and bulky CF_3 groups inhibit efficient chain packing and reduce local segmental mobility [1,2,4,6–10], therefore these types of materials tend to have a high free volume and high selectivity for gas separation. In addition, 6FDA-based polyimides usually have good solubility in common organic solvents and possess good mechanical and thermal properties, which are required for the fabrication of gas separation membranes [11–14].

The objective of this paper is to investigate the inherent gas permeation properties of a series of aromatic polyimides containing laterally attached *p*-terphenyls and biphenyls and to characterize the effects of pressure and temperature on their gas permeability, diffusion coefficients, and solubility coefficients. The *p*-terphenyl unit was chosen because the *p*-terphenyl group is a non-coplanar component in which the equilibrium inter-ring torsions are in the range of 40–50°. In principle, bulky substitutents are introduced to the middle benzene ring; it will produce higher levels of ring-torsion, and thus induce non-coplanar structure. The non-coplanar *p*-terphenyl and biphenyl groups would push the neighboring chains apart, resulting in a greater free volume and high permeability.

* Corresponding author. Fax: +65-6779-1936.
E-mail address: chencts@nus.edu.sg (T.S. Chung).

0032-3861/03/$ - see front matter © 2003 Elsevier Science Ltd. All rights reserved.
doi:10.1016/S0032-3861(03)00430-0

2. Experimental

2.1. Materials

4,4′-(Hexafluoroisopropylidene)diphthalic anhydride (6FDA; Aldrich) and 1,4-bis-(4-aminophenoxy) benzene (diamine **1** in Fig. 1) (TCI) were purified by sublimation under high vacuum. 1-Methyl-2-pyrrolidinone (NMP) was refluxed with calcium hydride for 3 h and then distilled off under vacuum. Acetic anhydride was used as freshly distilled, and triethylamine was treated with KOH pellets at reflux and then distilled off. All other solvents were obtained from various commercial sources and used without further purification. 2,5-bis(4-aminophenoxy) biphenyl (diamine **2** in Fig. 1) and 2′,5′-bis(4-aminophenoxy)-[1,1′;4′,1″] terphenyl (diamine **3** in Fig. 1) were synthesized according to the reported method [15,16]. Helium (He), hydrogen (H_2), oxygen (O_2), nitrogen (N_2), carbon dioxide (CO_2), and methane (CH_4) were obtained from SOXAL. The purity of CO_2 and O_2 is 99.8%, and the others are 99.995%. All the gases were used without further purification.

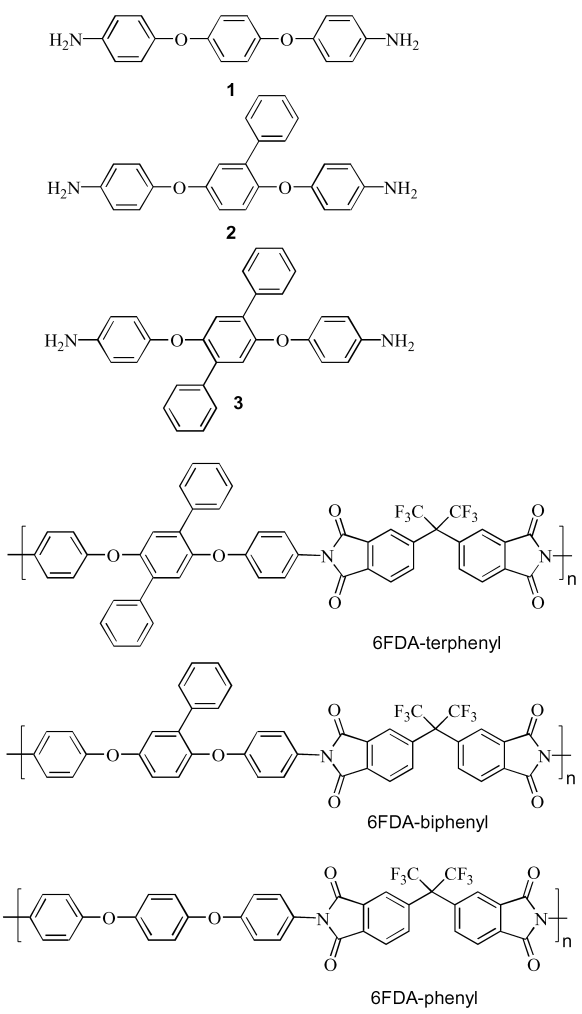

Fig. 1. Chemical structures of diamines and 6FDA-polyimides.

Polyimides were synthesized by a conventional two-step process involving the formation of polyamic acids followed by chemical dehydration to the polyimides in the presence of acetic anhydride and triethylamine in NMP at room temperature. The resulting viscous mixtures were slowly poured to methanol to yield the corresponding polyimides. The polyimides were washed with methanol, water and methanol again. Finally, the polyimides were redissolved in NMP, precipitated two times in methanol and dried in vacuum. Fig. 1 shows their chemical structures. The molecular weights of 6FDA-terpheyl, 6FDA-biphenyl and 6FDA-phenyl, measured by gel permeation chromatography on a Waters 2690 and using polystyrene as reference, are 95,000, 208,000 and 150,000, respectively, with a corresponding polydispersity of 2.4, 2.23, and 1.75.

2.2. Dense membrane preparation

The polyimides were first dissolved in THF to cast a dense yellowish polymeric film after evaporation in the fume hood for more than 5 days. However, the films obtained are opaque due to fast water absorption of THF. A clear film was finally obtained using dichloromethane as the solvent. Dense flat films were prepared by casting a methylene chloride solution containing about 2 wt% polymer on glass plates. Films were then dried at temperature which is higher than the boiling point of the solvent used for casting by 20 °C. For example, the films cast in methylene chloride were dried in an oven at 60 °C for 24 h (without vacuum) and at 60 °C with vacuum to remove residual solvent for another 24 h. The temperature was gradually increased at a heating rate of 12 °C/20 min from 60 to 250 °C, and each membrane was annealed at 250 °C for 24 h. The films were slowly cooled in an oven from 250 °C to room temperature over a period of several hours, then were stored in a desiccator for further tests. 6FDA-biphenyl films were cast in a heated oven at 75 °C in DMF, and then we follow the similar procedure as mentioned above. The casting and drying protocol has been established and reported by Chung and his group [8,17]. The typical thickness of the polymer films used in the present study is in the range of 38–42 μm.

2.3. Measurements of permeability and permselectivity

The permeability coefficients, P, and the apparent diffusion coefficients, D, were measured and calculated by the constant volume and vacuum time-lag methods [18], respectively. The permeability was determined in the sequence of He, H_2, O_2, N_2, CH_4, and CO_2. For He and H_2, the permeability were measured at 35 °C and 3.5 atm, while for other gases, they were tested from 35 to 50 °C at 10 atm. The design of permeation apparatus and detailed experimental procedure were described elsewhere [19]. In short, the gas permeability was determined from the rate of pressure increase (dp/dt) in the permeation (downstream)

side at the steady state using the following equation:

$$P = \frac{273}{76}\frac{VL}{ATp_0}\frac{\mathrm{d}p(t)}{\mathrm{d}t} \quad (1)$$

Where P is the permeability coefficient of a membrane to gas i and its unit is Barrer (1 Barrer $= 1 \times 10^{-10}$ cm^3(STP)-cm/cm^2-sec-cm Hg.), V is the volume of the low-pressure chamber, A is the effective area of the film, L is the thickness of the membrane, p_0 is the pressure in cm of Hg of the penetrant gas in the upstream chamber, T is the absolute temperature of the measurement, and $\mathrm{d}p(t)/\mathrm{d}t$ is the rate of pressure increase measured by a pressure transducer in the low-pressure chamber

The apparent diffusion coefficient was calculated from the time lag (θ) as follows:

$$D_{\mathrm{app}} = \frac{L^2}{6\theta} \quad (2)$$

Once P and D were calculated, the apparent solubility coefficient, S, was evaluated by means of the following expression:

$$S_{\mathrm{app}} = \frac{P}{D} \quad (3)$$

The units of D_{app} and S_{app} are cm^2/s and cm^3(STP)/cm^3-cmHg, respectively. The ideal separation factor of a membrane for gas A to gas B is defined as follows:

$$\alpha_{\mathrm{A/B}} = \frac{P_{\mathrm{A}}}{P_{\mathrm{B}}} \quad (4)$$

The relationships between permeability, diffusivitiy, and solubility with temperature are assumed to obey the Arrhenius equation as follows:

$$P = P_0 \exp\left(\frac{-E_{\mathrm{p}}}{RT}\right) \quad (5)$$

$$D = D_0 \exp\left(\frac{-E_{\mathrm{d}}}{RT}\right) \quad (6)$$

$$S = S_0 \exp\left(\frac{-H_{\mathrm{s}}}{RT}\right) \quad (7)$$

Where P_0 is a pre-exponential factor, E_{p} the activation energy for permeation, R the universal gas constant, and T the absolute temperature. D_0 is a pre-exponential factor and E_{d} the activation energy for diffusion. S_0 is a pre-exponential factor and H_{s} is the apparent heat of sorption.

2.4. Wide-angle X-ray diffraction

A wide-angle X-ray diffractometer (GADDS XRD system, Bruker AXS) were employed to determine the d-space of newly synthesized polymers using the Cu K_α radiation wavelength. The center of the broad peak on each X-ray pattern was attributed to the average intersegmental distance of polymer chains. The d-spacing is calculated by substituting the scattering angles (2θ) of the peak into the Bragg's equation, namely

$$n\lambda = 2d \sin\theta \quad (9)$$

where, θ was the X-ray diffraction angle and $\lambda = 1.54$ Å.

2.5. Density and fraction free volume

Film density was measured using a top-loading electronic Mettler Toledo balance with a density kit according to the Archimedean principle and by weighing samples in air and ethanol at room temperature. The volume of the sample was calculated from the weight difference of the measurements divided by the density of ethanol. From the weight in air and the calculated volume, film density was determined.

The fraction free volume (FFV) is calculated by the following equation:

$$\mathrm{FFV} = (V - V_0)/V \quad (10)$$

where V is the volume of polymer calculated from the measured density and V_0 is the occupied volume calculated from the correlation, $V_0 = 1.3V_{\mathrm{w}}$ where V_{w} is the van der Waals volume, which is estimated using the Bondi's group contribution method [20,21]. The specific free volume, $V_{\mathrm{f}} = (V - V_0)$, is defined as the difference between the observed specific volume, V, and the occupied volume V_0. Both FFV and the specific free volume are useful guides for interpreting permeation characteristics.

2.6. Dielectric properties

The films used for relative permittivity determination were coated with gold on a JEOL JFC-1200 fine coater. Relative permittivity was measured on a TA instruments DEA 2970 Dielectric Analyzer by the sputter coater method in the frequency range of 1–100 kHz on thin films.

3. Results and discussion

3.1. Gas transport properties vs. polymer structures

Table 1 summarizes and compares He, H_2, O_2, N_2, CH_4, and CO_2 permeabilities of this series of polyimides measured at 10 atm and 35 °C. It is clear that the permeabilities of polyimides correlate their structures. Since p-terphenyl part is relative rigid and longer, which may produce a higher level of ring-torsion than that of biphenyl, terphenyl-containing polyimide yields a much higher percentage of permeability increase than biphenyl-containing one. In addition, the percentage of permeability increase varies from gas to gas. In the case 6FDA-terphenyl vs. 6FDA-phenyl, the percentage of permeation increase is 18% for He (kinetic diameter of 2.6 Å), 36.3 % for H_2 (2.89 Å), 80.6% for CO_2 (3.3 Å), 62.8% for O_2 (3.46 Å), 81.2% for N_2 (3.64 Å), and 112% for CH_4 (3.8 Å). The percentage of permeatsion increment is highly dependent on

Table 1
A comparison of permeability at 35 °C and 10 atm

	Permeability (Barrer)						Ideal selectivity			
	He	H_2	O_2	N_2	CH_4	CO_2	CO_2/CH_4	CO_2/N_2	O_2/N_2	He/N_2
6FDA-terphenyl[a]	43.01	45.64	5.26	1.02	0.747	21.48	28.76	21.06	5.16	42.17
6FDA-biphenyl[b]	37.59	34.28	3.46	0.616	0.358	12.97	36.23	21.06	5.62	61.02
6FDA-phenyl[a]	36.45	33.49	3.23	0.563	0.353	11.89	33.68	21.12	5.74	64.74
Percentage of increase (6FDA-terphenyl vs. 6FDA-phenyl)	18	36.3	62.8	81.2	112	80.6				
Percentage of increase (6FDA-biphenyl vs. 6FDA-phenyl)	3.1	2.6	7.1	9.4	1.4	9.1				

[a] Cast from dichloromethane solutions.
[b] Cast from DMF solutions and dried in an oven at 75 °C.

the size of gas employed. For instance, the smallest He gas has the smallest percentage of permeation increment, whereas the biggest CH_4 molecule has the largest the percentage of permeation increment. Since He and H_2 are small molecules, they can diffuse through the polymers easily, and thus the effect of structure change on their permeation increments is relatively small as expected. The large increments in N_2 and CH_4 permeabilities suggest that the terphenyl moiety significantly hinders polyimide chain packing, as a consequence, it creates additional interstitial chain space and alters the free volume distribution for gas diffusion. Table 2 expresses permeability in terms of apparent diffusion coefficient and apparent solubility. The data show that the most gain in permeability for 6FDA-terphenyl polyimide arises from the enhancement in apparent diffusion coefficient.

However, in comparison with 6FDA-terphenyl, the permeability increase for 6FDA-biphenyl is very minor. This is probably because the additional phenyl groups imbed within the interstitial chain space and the space filling effect of the phenyl groups contributes to the decreased diffusion coefficients. As a result, some gases show negative increments in apparent diffusion coefficients as shown in Table 2. By analyzing the changes in apparent diffusion coefficient and solubility in Table 2, one may conclude that the permeability increase in 6FDA-biphenyl is mainly due to the increase in solubility.

As expected, the permselectivity for gas pairs of He/N_2, O_2/N_2, and CO_2/N_2 decreases with an increase in the number of attached phenyl group. Significant drops of permselectivity for He/N_2 and CO_2/CH_4 by 34.9 and 14.6%, respectively, are observed for 6FDA-terphenyl polyimide because of the rigidity and high aspect ratio of the terphenyl unit. It is interesting to notice that 6FDA-biphenyl has the highest CO_2/CH_4 permselectivity in these three polyimides possibly due to unique combined effects of free volume distribution and molecular interaction between the attached phenyl moiety and absorbed gases.

Table 3 summarizes density, FFV calculation, dielectric constant and d-spacing of these materials. The change of FFV, permittivity (dielectric constant) and density are consistent with the gain or loss of permeability from 6FDA-terphenyl to 6FDA-phenyl, indicating that the polymimide structures have an important effect on the permeability. The XRD diagrams of three polymimides are shown in Fig. 2. Since there are no well-defined peaks in the XRD diagram, all polyimides are amorphous, but exhibit a bit different patterns. The diffuse peaks around $2\theta \sim 20°$ correspond to coherent scattering between the molecular chains. In general, the gas permeability is also related to the morphology of polymer for example, amorphous membrane has considerably higher gas permeability than semi-crystalline polymer membrane. In fact somewhat different diffraction patterns for three polyimides gave us an indication that apart from the overall free volume and free volume distribution resulted from the structural difference in the series of polyimides, the morphological changes are also in part attributable to the change in gas permeability.

3.2. Temperature effects on the gas transport properties

The effect of temperature on permeabilities, diffusion coefficients and solubility coefficients of O_2, N_2, CH_4, and CO_2 for 6FDA-terphenyl polyimide was investigated under

Table 2
A comparison of apparent diffusivity and solubility coefficients at 35 °C and 10 atm

	Apparent diffusion coefficient (10^{-8} cm^2/sec)				Apparent solubility (10^{-3} cm^3(STP)/cm^3 cmHg)			
	O_2	N_2	CH_4	CO_2	O_2	N_2	CH_4	CO_2
6FDA-terphenyl	6.16	1.66	0.372	3.37	8.54	6.11	20.0	63.7
6FDA-biphenyl	4.23	1.00	0.192	2.01	8.19	6.15	18.7	64.6
6FDA-phenyl	4.40	1.05	0.192	1.97	7.34	5.35	18.4	60.3
Percentage of increase (6FDA-terphenyl vs. 6FDA-phenyl)	40.0	58.1	93.8	71.1	16.3	14.2	8.7	40.0
Percentage of increase (6FDA-biphenyl vs. 6FDA-phenyl)	−3.9	−4.8	0.0	2.0	11.6	15.0	1.6	6.7

Table 3
A comparison of density, FFV, TG, d-spacing and dielectric constant

	Density (g/cm^3)	FFV (%)	d-spacing (Å)	Dielectric constant (1 Hz)
6FDA-terphenyl	1.324	17.12	5.48	2.54
6FDA-biphenyl	1.366	15.55	5.51	2.56
6FDA-phenyl	1.412	15.14	5.49	2.82

an upstream pressure of 10 atm. As shown in Figs. 3(a) and 4(a), the gas permeabilities and diffusivities increase with an increase in temperature. As gas diffusion in polymers is an activated process, the diffusion coefficient will increases with the increase of temperature, thus yielding positive activation energy (E_d) for diffusion. Fig. 4(b) shows that gas solubility decreases with an increase in temperature, resulting in a negative heat of sorption (H_s). The temperature dependency of permeability is a combination of temperature dependencies of the diffusion and sorption. Since $E_d + H_s > 0$ as shown in Table 4, in other words, the diffusion coefficient is a stronger function of temperature than the solubility coefficient, hence, gas permeability increases with temperature.

Table 4 summarizes the calculated apparent activation energies of O_2, N_2, CH_4, and CO_2 for permeation and diffusion based on the Arrhenius plots. It can be seen that the activation energies of permeability and diffusion (E_p and E_d) increase with an increase in the kinetic diameter of a penetrant gas, and are in the order of CO_2 (3.30 Å), O_2 (3.46 Å), N_2 (3.64 Å), and CH_4 (3.80 Å).

Although permeability coefficients increase with temperature, permselectivities for gas pairs of He/N_2, O_2/N_2, CO_2/N_2, and CO_2/CH_4 decrease due to differences in permeation activation energies for various gas pairs as presented in Fig. 3(b). In most cases, the larger penetrant it exhibits, the greater the activation energy is for permeation as shown in Table 4. Thus, an increase in temperature leads to a higher percentage of permeability increase for a larger penetrant (a slow gas) than for a small penetrant (a fast gas), which consequently reduces the permselectivity. The

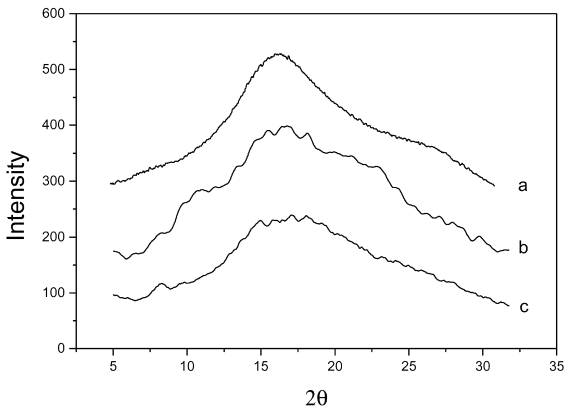

Fig. 2. The XRD diagram of polyimides (Intensity is offset for clarity) (a) 6FDA-phenyl, (b) 6FDA-biphenyl and (c) 6FDA-terphenyl.

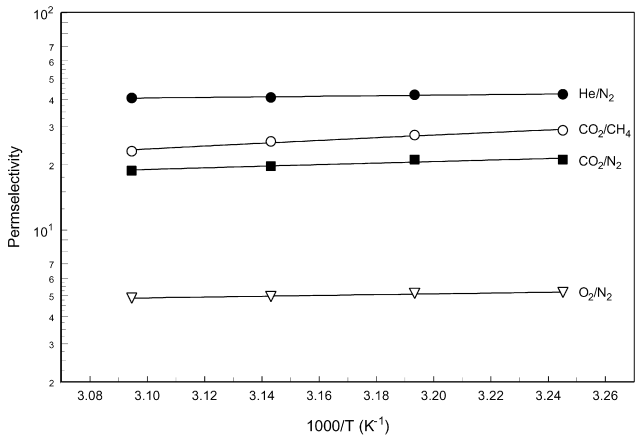

(a)

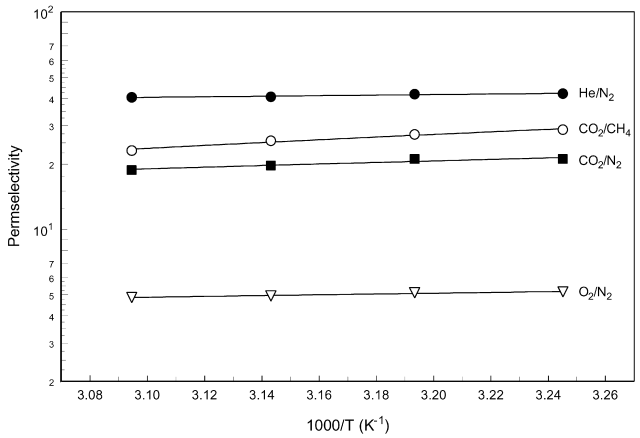

(b)

Fig. 3. Permeability and permselectivity as a function of temperature for 6FDA-terphenyl membranes. (a) Temperature dependence on permeability and (b) Temperature dependence on permselectivity.

temperature dependence of permselectivity is quantitatively determined by the difference in activation energies, $\Delta E_{p,A,B}$ of the A and B penetrants. A negative $\Delta E_{p,A,B}$ indicates a decrease in permselectivity.

3.3. Effect of the penetrant size on diffusivity

The Lennard-Jones collision diameter has been widely accepted to correlate diffusivities in relatively high mobility rubber or liquid media [22–24]. The kinetic diameter is close to the molecular sieving dimension of a gas and is a

Table 4
Activation energies of permeation and diffusion for 6FDA-terphenyl membranes at 10 atm

	O_2	N_2	CH_4	CO_2
E_p (kJ/mol)	9.91	13.41	18.63	6.50
E_d (kJ/mol)	25.52	30.03	35.02	22.51
H_s (kcal/mol)	−15.61	−16.62	−16.39	−16.01

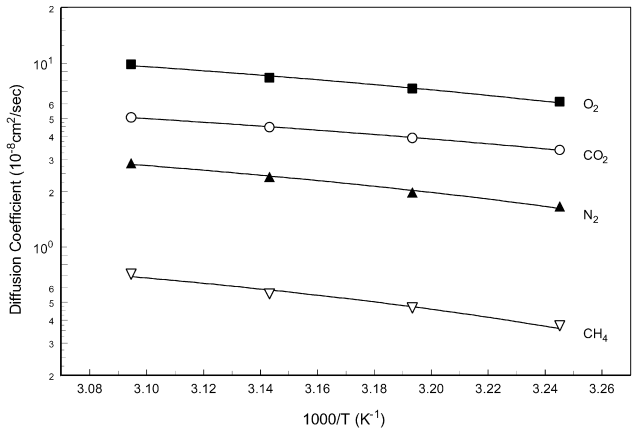

(a)

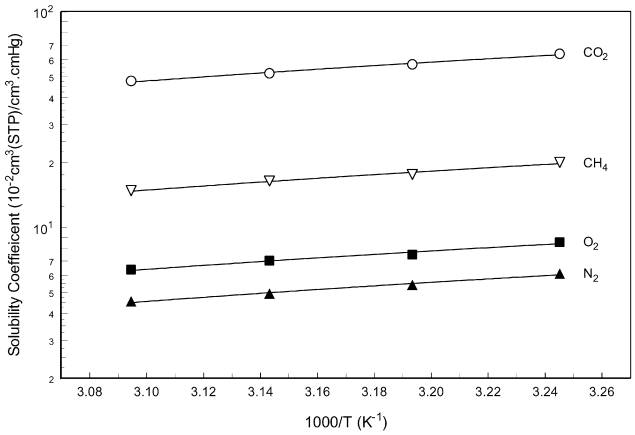

(b)

Fig. 4. Diffusivity and solubility as a function of temperature of 6FDA-terphenyl membranes (10 atm). (a) Temperature dependence on diffusion coefficients and (b) Temperature dependence on solubility coefficients.

sensitive measure of ability to move in highly restrictive environments. The values of the kinetic (σ_k) and collision (σ_c) diameters for various gases are similar to each other for most gases except for the case of CO_2, because the CO_2 molecule is linear and has strong molecular interaction. Fig. 5 shows a plot of gas diffusivity vs. square value of kinetic diameter. A straight line was drawn through the data points as visual aids only. It shows that only the CO_2 data point deviates significantly from this straight line and in an opposite way for the two gas diameters. Thus, following Shieh and Chung [19] work, an effective gas molecule diameter, which is defined as a square root of the product of gas collision and kinetic diameters, $\sigma_{\text{eff}} = \sqrt{\sigma_c \sigma_k}$ was used to correlate the CO_2 diffusivity. The deviation is significantly reduced.

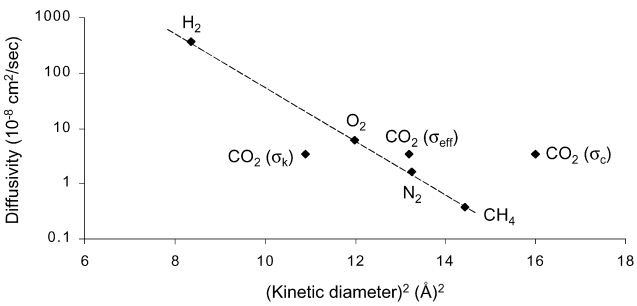

Fig. 5. Diffusivity as a function of the square of kinetic diameter of gas molecules for FDA-terphenyl polyimide at 35 °C.

3.4. Effect of the penetrant interaction or condensability on solubility

The following equation has been derived to correlate the gas solubility in polymer with T_c (critical temperature) or ϵ/k (Lennard-Jones force constant) and is expressed as [3]:

$$\ln S = \ln S_0 + K_c T_c \text{ or } = \ln S_0 + K_e(\epsilon/k) \quad (11)$$

where S_0, K_c, and K_e are constants. The gas solubility in this series of 6FDA-polyimides as a function of T_c is shown in Fig. 6 and the trend agrees with Eq. (11), i.e. the solubility increases as T_c increases. A similar conclusion can be made from the solubility vs. ϵ/k curve. Physically, T_c is a measure of the ease of condensation for gaseous molecules and ϵ/k is an indication of molecular interaction. It suggests that the more condensable or stronger molecular interaction the gas is, the higher the gas solubility is.

4. Conclusion

We have synthesized polyimides with a laterally attached phenyl moiety and determined their effect on gas permeability and selectivity. Only *p*-terphenyl polyimide exhibits a substantial increase in permeability because its terphenyl moiety is a rigid structure with a high aspect ratio. The attached phenyl moiety in 6FDA-biphenyl polyimide may imbed among the interstitial chain space, resulting in reduction in diffusion coefficients for some gases. The pattern of permeability increase from 6FDA-phenyl to 6FDA-terphenyl is in agreement with the pattern of

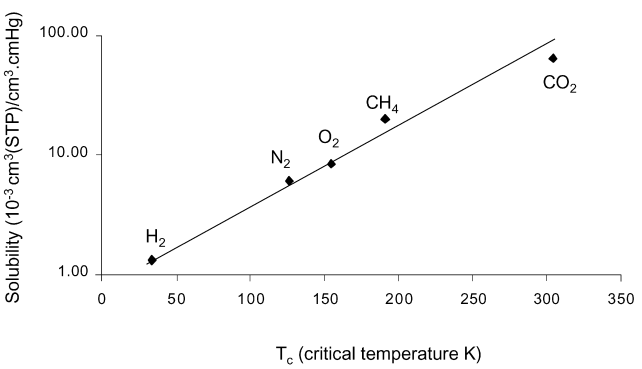

Fig. 6. Solubility as a function of critical temperature (T_c) for the 6FDA-terphenyl polyimide at 35 °C.

permittivity decrease. Besides the overall free volume and free volume distribution, the morphological changes of polymers as evidenced by XRD pattern play a role in affecting the gas permeation. The study also reveals that both diffusivity vs. gas penetrant size and gas solubility vs. critical temperature of gas penetrant follow a semi-log relationship.

Acknowledgements

The authors would like to thank Institute of Materials Research and Engineering (IMRE) for their financial support. Part of this work is also funded by the National University of Singapore (NUS) with the grant number of R-279-000-108-112. Special thanks are due to Dr Songlin Liu for his assistance on gas permeation tests and Dr K.P. Pramoda for her assistance on XRD measurements.

References

[1] Ohya H, Kudryavtsev VV, Semenova SI. Polyimide membranes: application, fabrications, and properties. Tokyo: Gordon and Breach Publishers; 1996.
[2] Koros WJ, Fleming GK, Jordan SM, Kim TH, Hoehn HH. Prog Polym Sci 1988;13(4):339–401.
[3] Paul DR, Yampol'skii YP. Polymeric gas separation membranes. Boca Raton: CRC Press; 1994.
[4] Stern SA. J Membr Sci 1994;94(1–3):1–65.
[5] Hirayama Y, Yoshinaga T, Kusuki Y, Ninomiya K, Sakakibara T, Tamari T. J Membr Sci 1996;111(2):169–82.
[6] Coleman MR, Koros WJ. J Polym Sci, Part B: Polym Phys 1994; 32(11):1915–26.
[7] Mi Y, Stern SA, Trohalaki S. J Membr Sci 1993;77(1):41–8.
[8] Lin WH, Vora RH, Chung TS. J Polym Sci, Part B: Polym Phys 2000; 38(21):2703–13.
[9] Robeson LM. J Membr Sci 1991;62(2):165–85.
[10] Freeman BD. Macromolecules 1999;32(2):375–80.
[11] Chung TS, Kafchinski ER, Foley P. J Membr Sci 1992;75(1–2): 181–95.
[12] Niwa M, Kawakami H, Nagaoka S, Kanamori T, Shinbo T. J Membr Sci 2000;171(2):253–61.
[13] Wang R, Cao YM, Vora RH, Tucker RJ. J Appl Polym Sci 2001; 82(9):2166–73.
[14] Cao C, Wang R, Chung TS, Liu Y. J Membr Sci 2002;209(1):309–19.
[15] Xu JW, He CB, Chung TS. J Polym Sci, Part A: Polym Chem 2001; 39(17):2998–3007.
[16] Xu JW, He CB, Wei TS, Chung TS. Plast Rubber Compos 2002;31(7): 295–8.
[17] Chung TS, Chan SS, Wang R, Lu ZH, He CB. J Membr Sci 2003; 211(1):91–9.
[18] Koros WJ, Paul DR. J Polym Sci, Part B: Polym Phys 1976;14(10): 1903–7.
[19] Shieh JJ, Chung TS. J Polym Sci, Part B: Polym Phys 1999;37(20): 2851–61.
[20] Bondi A. J Phys Chem 1964;68(3):441–51.
[21] Van Krevelen DW. Properties of polymers, 3rd ed. Amsterdam: Elsevier Science; 1990.
[22] Bird RB, Stewart WE, Lightfoot EN. Transport phenomena. New York: Wiley; 1960.
[23] Breck DW. Zeolite molecular sieves. New York: Wiley; 1974.
[24] Stannett V. Simple gases. In: Crank J, Park GS, editors. Diffusion in polymers. New York: Academic Press; 1968.